Solidification of ion exchange resins saturated with Na^+ ions: Comparison of matrices based on Portland and blast furnace slag cement

E. Lafond, C. Cau Dit Coumes, S. Gauffinet, D. Chartier, L. Stefan, P. Le Bescop

Solidification of ion exchange resins saturated with Na^+ ions: comparison of matrices based on Portland and blast furnace slag cement

E. LAFOND[1], C. CAU DIT COUMES[1], S. GAUFFINET[2*], D. CHARTIER[1], L. STEFAN[4], P. LE BESCOP[3]

[1] CEA, DEN, DTCD, SPDE, F-30207 Bagnols-sur-Cèze cedex, France

[2] Laboratoire Interdisciplinaire Carnot de Bourgogne UMR 6303 CNRS-Université de Bourgogne, Dijon, France, 9 Av Alain Savary, BP 47870, 21078 Dijon cedex, France

[3] CEA, DEN, DPC, SECR, F-91192 Gif-sur-Yvette, France

[4]AREVA, Back End Business Group, Dismantling & Services, 1 place Jean Millier 92084 Paris La Défense, France

*Corresponding author: sandrine.gauffinet@u-bourgogne.fr

Abstract

Ion exchange resins (IERs) are widely used by the nuclear industry to decontaminate radioactive effluents. After use, they are usually stabilized and solidified by encapsulation in cementitious materials. However, for certain combinations of cement and resins, the solidified waste forms can exhibit strong expansion, possibly leading to cracking of the matrix.

In this work, the behaviour of cationic resins in the Na^+ form is investigated in Portland cement (CEM I) or blast furnace slag cement (CEM III/C) pastes at early age in order to have a better understanding of the swelling process. The results show that during the hydration of the CEM I paste, the resins exhibit a transient expansion of small magnitude due to the decrease in the osmotic pressure of the pore solution. This expansion, also observed with C_3S pastes containing similar IERs, occurs just after setting and is sufficient to damage the material which is poorly consolidated. In the CEM III/C paste, expansion of the resins occurs before the end of setting and only induces limited stress in the matrix which is still plastic.

Keywords : ion exchange resins, swelling, hydration, Portland cement, blast furnace slag cement

1. Introduction

Ion exchange resins (IERs) are commonly used by the nuclear industry in the decontamination process of radioactive effluents. The spent resins become a low-level or intermediate-level radioactive waste and have to be stabilized and solidified, i.e. placed under a solid, stable, monolithic and confining form, before being sent to disposal. Calcium silicate cements offer many advantages for resins encapsulation: easy supply, simple process, good mechanical strength, compatibility with aqueous wastes, good self-shielding, and high alkalinity which allows many radionuclides to be precipitated and thus confined. However, for certain combinations of cement and resins, the solidified waste forms can exhibit strong dimensional variation, possibly leading to cracking of the matrix.

Several specificities of IERs have to be taken into account to design a robust cement-based matrix, such as low intrinsic mechanical strength and possible ionic exchanges with the pore solution [1, 2]. It is also well known that in aqueous medium, the volume of IERs beads strongly depends on the composition of the solution. Expansion or shrinkage can be caused by ionic exchanges and/or variations in osmotic pressure. These volume changes can also occur in a cementitious matrix, the pore solution chemistry of which evolves with ongoing hydration and, under severe conditions, they can induce cracking of the matrix [3-5]. Knowledge about the chemical evolution of IERs in a cementitious environment is limited. For example, it is often mentioned in the literature that the encapsulation of IERs with Portland cement (CEM I) leads to strong expansion during the early stages of cement hydration, whereas no swelling is observed when Portland cement is blended with high amounts of blast furnace slag [6,7]. However, the reasons for these different behaviours are not understood.

To simplify the system under investigation, Portland cement was replaced in a previous study by its main component, tricalcium silicate [8]. The C_3S-waste form also exhibited a strong expansion and two main stages were observed during hydration at early age. In the first one, due to ionic exchange (fixation of calcium, release of sodium), the resins shrank. Then, in a second stage, as hydration accelerated, the sodium concentration in the pore solution rapidly decreased due to the precipitation of sodium-bearing C-S-H, whereas the resins continued to fix calcium ions. Swelling of the resins occurred during the second stage, and resulted from the decrease in the osmotic pressure of the pore

solution due to the consumption of sodium ions. Despite its small magnitude, swelling seemed to be enough to deteriorate the hardened matrix during the second stage, just after setting, while the degree of hydration was still low and the matrix poorly consolidated.

To provide deeper understanding of real systems, this work aims at comparing the hydration of Portland cement and blast furnace slag cement (CEM III/C) pastes with cationic resins initially in the Na^+ form. The objective is to explain why cements containing high amounts of blast furnace slag are more appropriate than Portland cement to solidify and stabilize this waste.

2. Experimental

2.1 Materials

The two cements used in this study were referred as CEM III/C (32.5 N from Calcia Rombas) and CEM I (52.5 N from Calcia Couvrot). According to European standard EN 197-1:2000, CEM I comprises 95-100% Portland Cement clinker whereas CEM III/C corresponds to a Blast Furnace Cement consisting of 5-19% Portland cement clinker and 81-95% blast furnace slag. The compositions of the cements and clinker are reported in Tables 1 and 2. The two cements comprised the same Portland clinker, but in different amounts.

IERs were supplied by Rohm&Haas under the trade name Amberlite IR120H in the physical form of spherical beads or ground grains. The IER beads had a diameter comprised between 620 and 830 µm, and the ground IERs had a particle size ranging from 0.4 µm to 300 µm (d_{10} = 15 µm, d_{50} = 65 µm, d_{90} = 155 µm). The exchange sites of the resins, shipped in the H^+ form, were saturated with Na^+ ions by percolating a solution of sodium hydroxide. The pH of the eluted solution was continuously monitored, and the percolation was stopped as soon as the pH exceeded 7. The resins were then rinsed with water to eliminate the excess of base and to recover a neutral pH. Finally, the suspension of water and resins was filtered under humid atmosphere and slight vacuum on a Buchner funnel to remove the free intergranular water (water between the resin grains). The dry extract of the wet resins was measured by gentle heating at 55°C (to avoid any damage of the functional groups) until constant

weight. Values of 54.3 ± 0.2 % and 45.3 ± 0.2 %. were achieved for beads and ground grains respectively. This difference was explained by the fact that ground resins developed a larger surface area than bead resins. The volume of water adsorbed onto the surface of resin was thus more important. The wet resins were kept in tightly closed containers. The resins were used in their ground form, except for SEM observations where beads were preferred.

2.2 Preparation of samples

Experiments were conducted on pure cement pastes, consisting of CEM III/C or CEM I cement and water, as well as on cement pastes mixed with IERs.

To prepare pure cement pastes, CEM III/C or CEM I cements were introduced in a standardized laboratory mixer (European Standard EN 196-1) with water, mixed at low speed for 30 s and at high speed for 3 min. The water-to-cement ratio was fixed to 0.55, which corresponded to the effective water-to-cement ratio of the pastes with IERs, calculated by correcting the total amount of water from that retained in the IERs to solvate the ionic groups. This latter was assessed by measuring their dry extract after the saturation step with Na^+ ions, as previously explained in section 2.1. The pure cement pastes exhibited transient bleeding which disappeared after setting.

Mixing of cement/IERs systems was performed in two steps: IERs and water were first stirred during 30 s at low speed in a standardized laboratory mixer. Then, cement (CEM I or CEM III/C) was introduced in the mixer, mixed at low speed for 30 s and at high speed for 3 min. Samples contained 11 wt. % of dry resins, and a total water-to-cement ratio of 0.8. The high water content enabled to get workable grouts and ensured that the system remained saturated, at least at early age.

The fresh grout samples were cast into hermetically sealed 50 mL-polypropylene containers and stored in a climatic chamber at 20°C with 95% relative humidity until characterization.

2.3 Characterization of hydration

The Vicat setting time was measured using an automatic Vicat needle apparatus according to EN 196-3 standard. In addition, to point out the different stages of hydration, calorimetric measurements were carried out using isothermal microcalorimetry at 25°C (SETARAM, C80 type). Hydration was also stopped after fixed periods of time (from 1 hour to 10 days) by successively immersing the crushed pastes into isopropanol and drying them in a controlled humidity chamber (with 20% relative humidity at 22 ± 2°C). After grinding to a particle size below 80 µm, the mineralogy of the cement pastes was characterized by X-ray diffraction (Siemens D8, copper anode, $\lambda_{K\alpha 1}$=1.54056 Å,). A semi-quantitative analysis was performed to assess the evolution of the amounts of reactants and products with time using EVA analysis software (© 2005 Bruker AXS). The method consisted in introducing an internal standard (10 wt% silicon, correction made to take into account the increasing amount of bound water with ongoing hydration) into the sample to be analysed by XRD, and then in calculating the ratio between the area of the most intense diffraction peak of the phase to quantify and that of silicon. The microstructure evolution was observed by Scanning Electron Microscopy (FEI Inspect S50, high vacuum mode, acceleration voltage of 15 kV, current intensity of 50 nA) on sample fractures and polished section at different ages. The Na/S, Ca/S, Na/Si and Ca/Si ratios in the hydrates and IER grains were determined by X-ray microanalysis on polished cross sections (high vacuum mode, Bruker SDD detector calibrated on jadeite, FeS_2 and wollastonite).

The pore solutions of cement pastes were extracted using pressure (34 MPa) from 1 hour to 10 days. The Na^+, K^+, Ca^{2+}, and SO_4^{2-} concentrations were determined using ionic chromatography (Dionex DX500 equipped with IonPac CS12A analytical column and IonPac CG12A guard column). The analytical error was ± 5%.

2.4 Characterisation of volumetric change

The shrinkage cone method was used to follow the apparent volumetric change of cement-waste forms with ongoing hydration. It was initially developed by the German Cement Works Association for measuring the autogenous shrinkage of concrete [9]. The setup (from Schleibinger Geräte) consisted of a laser vertically pointed at the surface of a cone-shaped sample in a cylindrical jar

connected to a thermostatic bath at 25°C. The sample was poured into the jar and slightly vibrated. The surface of the sample was covered with a plastic sheet equipped with a reflector to avoid desiccation. The jar was then placed underneath the laser, and the distance variation between the reflector and the laser was recorded every 10 minutes. The measurement range was 5 mm, with a resolution of 0.1 µm. The cone geometry ensured that the change in height corresponded to the linear length change of the material as long as it was fluid and also after solidification since deformation was considered as uniform.

Based on the work of Matsuda [4], an oedometric cell was developed to measure the swelling pressure induced by cemented resins under constrained environment. 20 g of paste samples were introduced in a cylindrical cell containing a metallic fritted disc at the bottom (Figure 1). A second fritted disc was placed on the upper surface sample and the cell was tightly closed with a piston connected to force sensor. An initial pressure of 0.1 MPa was applied. Measuring the increase in the axial stress enabled to follow the swelling pressure of samples with time.

3. Results

3.1 Volumetric change with ongoing hydration

Figure 2 shows the evolution of the swelling pressure of cement-IERs forms under constant strain. As expected, the pressure increased only for the CEM I sample. Tests with the shrinkage cone showed that, under unconfined conditions, this sample also exhibited a strong apparent volume increase which began 8 h after mixing and exceeded 7% after 220 h.

3.2 Characterization of hydration

The Vicat setting time of the CEM I and CEM III/C cement pastes was measured with or without IERs in Na^+ form. The results are presented in Table 3. The presence of IERs tended to accelerate the setting of both cements. Setting started 30 min earlier, and ended from 1 h (CEM III/C) to 2.75 h

(CEM I) earlier than in the corresponding pure cement pastes. These results were consistent with the heat flow measurements (Figure 3), showing a slight acceleration of the heat production in the samples containing resins. The setting of the CEM III/C samples remained however much slower than that of the CEM I samples because of the low reactivity of blast furnace slag as indicated by the reduced heat production (Figure 3).

3.3 Pore solution evolution

Figures 4 and 5 show the evolution of the pore solution composition and corresponding osmotic pressure (from 1 h to 10 d) for CEM I and CEM III/C paste samples with and without resins.

The osmotic pressure of the pore solution was calculated using Van't Hoff equation (1).

$$\pi = \Phi RT \sum_i c_i \quad (1)$$

where π is the osmotic pressure of the solution (Pa), ϕ the osmotic coefficient, R the constant of ideal gases (8.314 $J.mol^{-1}.K^{-1}$), T the temperature (K) and c_i the concentration of ion *i* in solution ($mol.L^{-1}$). The osmotic coefficient is a corrective factor taking into account the non-ideal behavior of the solution. It was calculated using PhreeQC [10] and Pitzer's thermodynamic database [11].

In both materials, the sodium concentration rapidly increased during the first 8 h and reached a maximum which corresponded to about 1/3 of the sodium initially fixed by the resins (35% for CEM I sample, 30% for CEM III/C sample). The potassium concentration was much lower than in the pure cement pastes. It was also the case for the calcium concentration, but to a lesser extent.

These results showed a partial exchange of Na^+ ions from the resins with Ca^{2+} and K^+ ions released by the dissolution of the cement anhydrous phases. In the same time, the sulphate concentration increased due to the dissolution of gypsum. As a result, the osmotic pressure of the pore solution also increased. From previous studies devoted to the volume change of IERs depending on their chemical environment [8, 12], it could be concluded that the $2Na^+ \leftrightarrow Ca^{2+}$ and $Na^+ \leftrightarrow K^+$ exchanges as well as the increase in the osmotic pressure should cause a shrinkage of the IERs during this period. K^+ ions have indeed a smaller solvated ionic radius (~3.2 Å) than Na^+ ions (~4.0 Å) [13]. As for calcium, its

167 solvation ionic radius is close to that of Na^+, but since it is a divalent cation, its concentration in the
168 resins is divided by a factor 2. Besides, when the osmotic pressure of the solution external to the
169 resins increases, water tends to get out of the resins to reduce the external concentration and
170 equilibrate the chemical potentials between the external and internal solutions.
171
172 Then, a second stage occurred. Sulphate ions were depleted from the interstitial solution due to the
173 precipitation of ettringite (the exhaustion of gypsum was also observed by XRD at the same time,
174 Figures 6 and 7). The sodium concentration in solution also decreased. As a consequence, the osmotic
175 pressure of the external solution diminished, which produced a swelling of the IERs [8, 12]. Its
176 magnitude was assessed using previously established calibration curves plotting the volume of Na^+-,
177 K^+-, and Ca^{2+}-IER beads versus the osmotic pressure of the external solution [8, 12, 14]. It was close
178 to 0.1 % for the IERs-CEM I sample, and 0.19 % for IERs-CEM III/C sample.
179
180 **3.4 IERs analysis**
181
182 X-ray microanalyses were performed on polished cross-sections of pastes with IER beads after 2 and
183 24 hours of hydration. For each hydration time, 10 IER grains were selected and more than 10
184 analyses were performed on each grain. The average Na/S, Ca/S and K/S ratios measured on samples
185 aged of 2 h and 24 h are given in Table 4. The results confirmed the fixation of Ca^{2+} and K^+ ions by
186 the resins during the early stages of hydration. The Na/S ratio continuously diminished with time.
187 Thus, the decrease in the sodium concentration observed in the pore solution after 8 h (CEM I) or 3 h
188 (CEM III/C) was not due to re-fixation of Na^+ ions on the resins, with simultaneous release of K^+ or
189 Ca^{2+} ions in solution.
190
191 **3.5 Mineralogy evolution**
192
193 The mineralogy of the different investigated systems was characterized by XRD and SEM. The CEM
194 I-based materials comprised C-S-H, portlandite, ettringite as well as residual anhydrous cement

phases (Figure 6). In the CEM III/C-based materials, the same hydrates were detected with the exception of portlandite (Figure 7). For a given type of cement, the resins did not change the nature of the precipitated hydrates, but only influenced their rate of formation (Figure 8).

In both cement-IERs systems, X-ray microanalysis performed on polished cross-sections of 24h-old samples showed that C-S-H sometimes comprised significant amounts of sodium. This sodium-bearing C-S-H was very heterogeneously distributed in the matrix, with an average Na/Si ratio close to 0.2 after 24 h. Its precipitation could explain the second decrease in the sodium concentration of the pore solution. The formation of both C-S-H and C-N-S-H has also been reported when resins in the Na^+ form are encapsulated in a C_3S paste [8], or during the hydration of blast-furnace slag activated by a concentrated NaOH solution [15].

SEM observations of fractures also confirmed the precipitation of portlandite in the IERs-CEM I sample, as big crystals of a few 100 µm (Figure 9-a) at the interface between IER grains and paste. This localized precipitation seemed consistent with the results presented in sections 3.3 and 3.4. The shrinkage of the resins in the first stage of hydration would create voids at the resin/paste interface where portlandite could precipitate. Besides, the strong affinity of the resins for calcium ions would induce a calcium flux from the paste to the resins, possibly leading to a local supersaturation with respect to portlandite near the resin beads. By contrast, in the IERs-CEM III/C samples, no portlandite precipitation was observed (Figure 9-b).

4. On the swelling of IERs-CEM I samples

The CEM I- and CEM III/C-based materials differed by their consolidation rate. When resins were encapsulated in the CEM III/C matrix, expansion occurred between the beginning and the end of Vicat setting, when the material was still plastic. The CEM I cement exhibited a higher rate of hydration, and swelling of the IERs occurred just a few hours after the Vicat end of setting, in a hardened matrix, but with:

- *(i)* low mechanical strength. As a fact, when calcium ions are progressively replaced by monovalent cations such as sodium ions, the cohesion decreases, and repulsion between C-S-H

particles can even be observed if the negative surface charge density is balanced by monovalent cations only [16, 17]. Precipitation of C-N-S-H in the pastes with Na^+-IERs could thus contribute to reduce the strength of the matrix.

- *(ii)* heterogeneous microstructure. Highly porous transition zones were observed between IER grains and the cement paste with precipitation of large crystals of portlandite.

Despite its small magnitude, the swelling of IERs due to the decrease in the osmotic pressure of the pore solution could be sufficient to induce cracking of the poorly consolidated matrix.

To check this assumption, complementary experiments were carried out on IERs-CEM I samples by retarding the setting without notable change in the chemical evolution. To this end, the fresh grout was divided in two samples which were cured at two different temperatures, 5 and 20 °C. The damage of the cement-resin forms was assessed qualitatively by visual observation (Table 5, Figure 10). Extractions of solutions were performed at 1 h, 5 h, 7 h, 24 h, 48 h and 7 d. The Vicat setting time was also measured at both temperatures. Results are reported in Figure 11.

The ionic concentrations showed very similar evolutions with time at both temperatures; the decrease in temperature thus did not affect significantly the chemical evolution of the systems at early age, showing that ionic exchanges on the resin grains, which are very fast, played a key role during this period. Decreasing the temperature however delayed the beginning and end of setting by 8.5 h. As observed before, at 20 °C, the end of setting occurred when the sodium concentration was at its maximum, corresponding to resins under their most contracted form. The slight expansion of the resins caused by the decrease in the osmotic pressure of the interstitial solution (exhibiting the same trend as the sodium concentration) took place just after setting, leading to cracking and disintegration of the sample. At 5°C, setting occurred once the resins had started to swell, and the damages were much less important. The consolidation rate thus seemed to be a key parameter to explain expansion and damage of IERs-CEM I materials.

5. Conclusions

The results show that during the hydration of CEM I and CEM III/C cement pastes, the resins exhibit a transient expansion of small magnitude due to the decrease in the osmotic pressure of the interstitial solution. This expansion occurs just after setting for IERs-CEM I forms. It is sufficient to damage the material which is poorly consolidated with heterogeneous microstructure. Expansion of the IERs-CEM III/C forms is not observed because CEM III/C cement exhibits a slower rate of hydration than CEM I cement. Transient expansion of the resins takes place before the end of setting and only induces limited stress in the material which is still plastic.

REFERENCES

[1] V. Morin, S. Garrault, F. Begarin, I. Dubois-Brugger, The influence of an ion-exchange resin on the kinetics of hydration of tricalcium silicate, Cem. Concr. Res. 40 (2010) 1459-1464.

[2] Q. Sun, J. Li, J. Wang, Solidification of borate radioactive resins using sulfoaluminate cement blended with zeolite, Nucl. Eng. Design 241 (2011) 5308-5315.

[3] P. Soo, L.W. Milian, The impact of LWR decontamination on solidification, waste disposal and associated occupational exposure. Effect of composition on the strength, swelling and water-immersion properties of cement-solidified ion-exchange resin wastes, Brookhaven National Laboratory, NUREG/CR-3444 (1991).

[4] M. Matsuda, M. Kikuchi, T. Takashi, Conditioning of spent ion exchange resin using high performance cement, Proc. Waste Management, Tucson, Arizona (1993).

[5] G.W. Veazey, R.L. Ames, Cement waste-form development for ion exchange resins at the Rocky Flats plant, Los Alamos National Laboratory, LA-13226-MS UC-721 (1997).

[6] M. Matsuda, T. Nishi, K. Chino, M. Kikuchi, Solidification of Spent Ion-Exchange Resin Using New Cementitious Material .1. Swelling Pressure of Ion-Exchange Resin, J. Nucl. Sci. Techn.(1992) 883-889.

[7] V.N Epimakhov, M.S Oleinik, Inclusion of radioactive ion-exchange resins in inorganic binders, Atomic Energy, 99 (2005) 607-611.

[8] E. Lafond, C. Cau Dit Coumes, S. Gauffinet, D. Chartier, P. Le Bescop, L. Stefan, A. Nonat, Investigation of the swelling behaviour of cationic exchange resins saturated with Na^+ ions in C_3S paste, Cem. Conc. Res. 69 (2015) 61-71.

[9] S. Eppers, C. Müller, The shrinkage cone method for measuring the autogenous shrinkage: an alternative to the corrugated tube method, Proc. International RILEM conference on the use of superabsorbent polymers and other new additives in concrete, Lyngby, Denmark (2010) 67-76.

[10] D.L. Parkurst, D.C. Thorstenson, L.N. Plummer, PHREEQC, A Computer Program for Geochemical Calculations: U.S. Geological Survey Water-Resources Investigations, Report 80–96, 195 (1980) (revised and reprinted August 1990).

[11] L.N. Plummer, D.L. Parkhurst, G.W. Flemming, S.A. Dunkle, A computer program incorporating Pitzer's equations for calculation of geochemical reactions in brines, US Geological Survey, Water-Resources Investigation Report 88 4153 (1988).

[12] E. Lafond, Etude chimique et dimensionnelle de résines échangeuses d'ions cationiques en milieu cimentaire, PhD thesis, Université de Bourgogne, France (2013).

[13] W. Rieman, H.F. Walton, Ion exchange in analytical chemistry, Pergamon Press, Oxford, Great Britain, (1970) 24-27.

[14] C. Cau Dit Coumes, E. Lafond, S. Gauffinet, D. Chartier, P. Le Bescop, L. Stefan, A. Nonat, On the swelling behavior of cationic exchange resins saturated with Na^+ ions in a C_3S or Portland cement paste, Proc. NUWCEM 2014, 3-6 juin, Avignon, France (2014).

[15] M. Ben Haha, G. Le Saout, F. Winnefeld, B. Lothenbach, Influence of activator type on hydration kinetics, hydrate assemblage and microstructural development of alkali activated blast furnace slags, Cem. Concr. Res. 41 (2011) 301-310.

[16] S. Lesko, Mesure des forces interparticulaires par microscopie à force atomique. Application à la cohésion des ciments, PhD thesis, Université de Bourgogne, France (2005).

[17] C. Labbez, B. Jonsson, I. Pochard, A. Nonat, B. Cabane, Surface charge density and electrokinetic potential of highly charged minerals: experimental and Monte Carlo simulations on calcium silicate hydrate, J. Chem. Phys. B. 110 (2006) 9219-9230.

304 Table 1: Composition of CEM I cement (oxide composition determined by X-ray fluorescence, phase

305 composition determined by Rietveld analysis).

	CaO	**SiO_2**	**Al_2O_3**	**Fe_2O_3**	**SO_3**	**K_2O**	**Na_2O**	**MgO**	**MnO**
Chemical composition of cement (wt.%)	64.44	20.42	5.21	2.33	3.68	1.14	0.89	1.07	0.04
Phase composition of clinker (wt.%)		C_3S: 66 C_2S: 13 C_3A: 11 C_4AF: 7		**Cement composition (wt.%)**			Clinker: 94% Gypsum: 6%		

306

307

Table 2: Composition of CEM III/C cement (oxide composition determined by X ray fluorescence, phase composition determined by Rietveld analysis).

	CaO	**SiO_2**	**Al_2O_3**	**Fe_2O_3**	**SO_3**	**K_2O**	**Na_2O**	**MgO**	**MnO**	**TiO_2**	**P_2O_5**
Chemical composition of cement (wt. %)	45.1	32.0	10.3	0.8	2.9	0.55	0.18	6.1	0.4	0.5	0.1
Phase composition of clinker (wt.%)		C_3S: 66 C_2S: 13 C_3A: 11 C_4AF: 7			**Cement composition (wt.%)**				Blast furnace slag: 80.5 Clinker: 14.2 Anhydrite: **5.2**		

312 Table 3: Vicat setting times of CEM I and CEM III/C cement pastes with and without IERs (± 0.3 h).

Sample	Beginning of setting (h)	End of setting (h)
CEM I	4.0	11.3
CEM I + IERs	3.5	8.5
CEM III/C	6.5	31.0
CEM III/C + IERs	6.0	30.0

313

314

315 Table 4: Na/S, Ca/S and K/S molar ratios of resin beads encapsulated in a CEM I or CEM III/C

316 cement paste.

Type of cement	Age of sample (h)	Na/S		Ca/S		K/S	
		Average	Standard deviation	Average	Standard deviation	Average	Standard deviation
CEM I	2	0.86	0.06	0.03	0.03	0.14	0.02
	24	0.78	0.05	0.07	0.02	0.19	0.01
CEM III/C	2	0.85	0.07	0.08	0.06	0.03	0.01
	24	0.79	0.07	0.10	0.06	0.04	0.01

317

318

319 Table 5: Visual observations of IERs-CEM I and IERs-CEM III/C samples cured at 25°C and 5°C.

Hydration time	25°C	5°C
3 days	Apparition of the first cracks	No cracks
6 days	Destruction of the container	Slight cracks on the container
10 days	Destruction of the sample	Slight cracks on the container

320

321

322 Figure 1: Experimental device to measure swelling pressure under constrained environment.

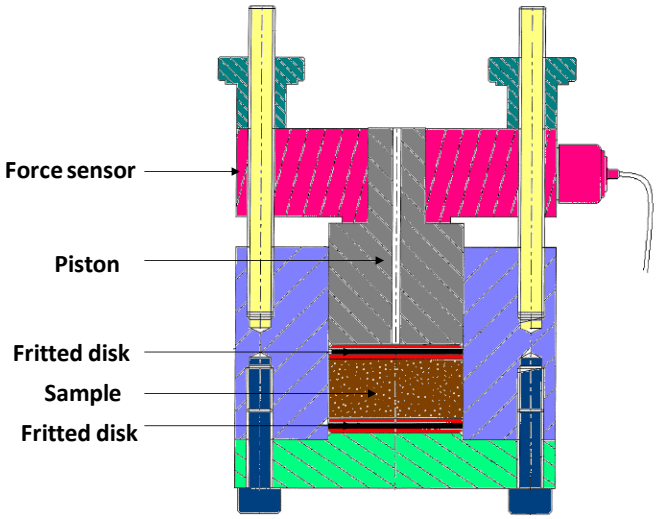

323

324

Figure 2: Evolution with time of the pressure induced by IERs-CEM I and IERs-CEM III/C samples under confined environment; comparison with their volumetric change under unconfined environment.

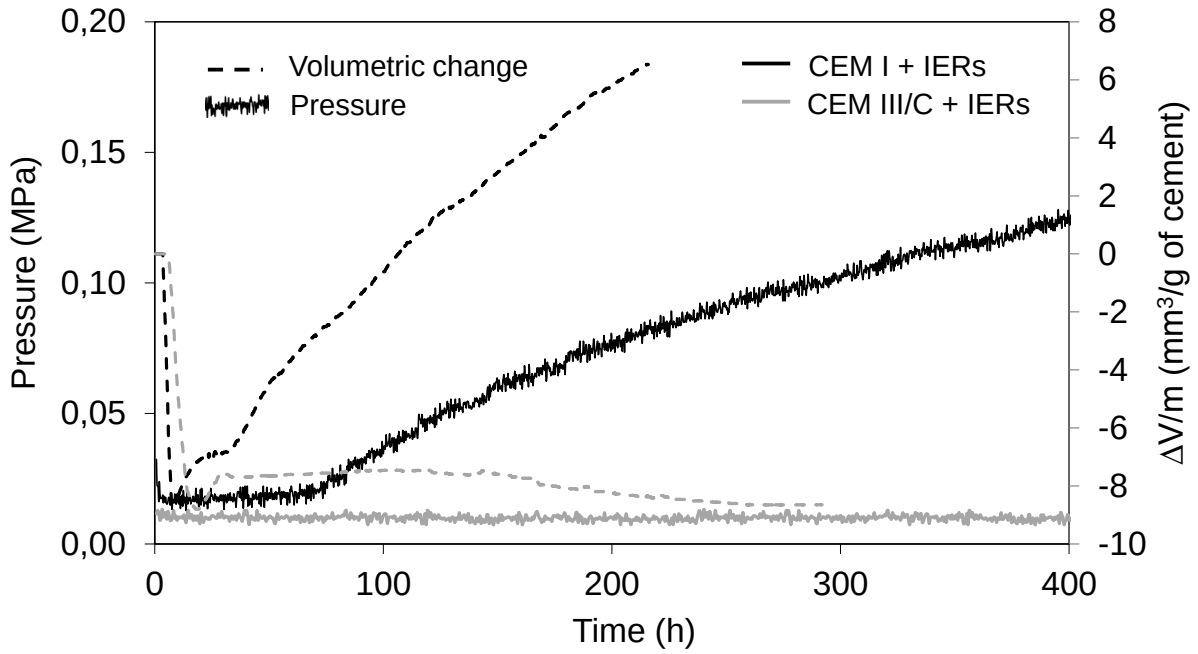

Figure 3: Cumulative heat flow versus time for CEM I and CEM III/C cement pastes with and without IERs.

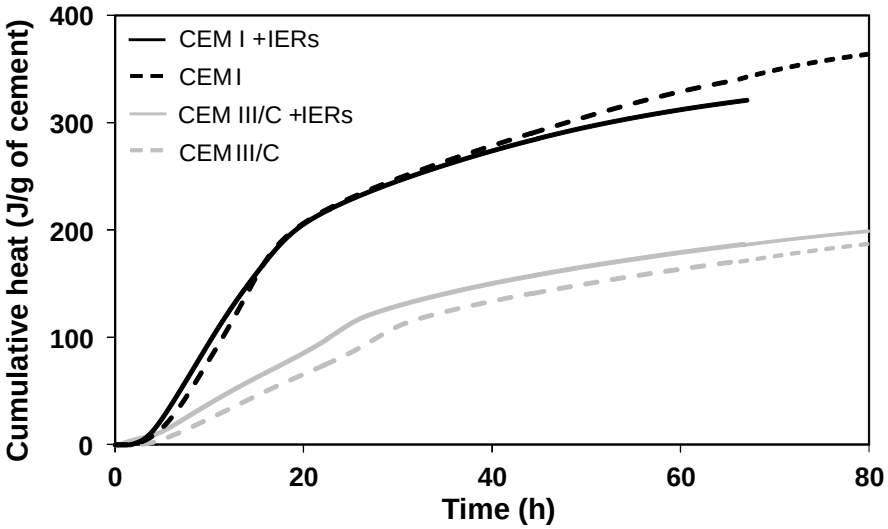

Figure 4: Evolution of the composition (Na^+, K^+, Ca^{2+}, SO_4^{2-}) and osmotic pressure of the interstitial solution of CEM I cement paste samples with (a) and without resins (b).

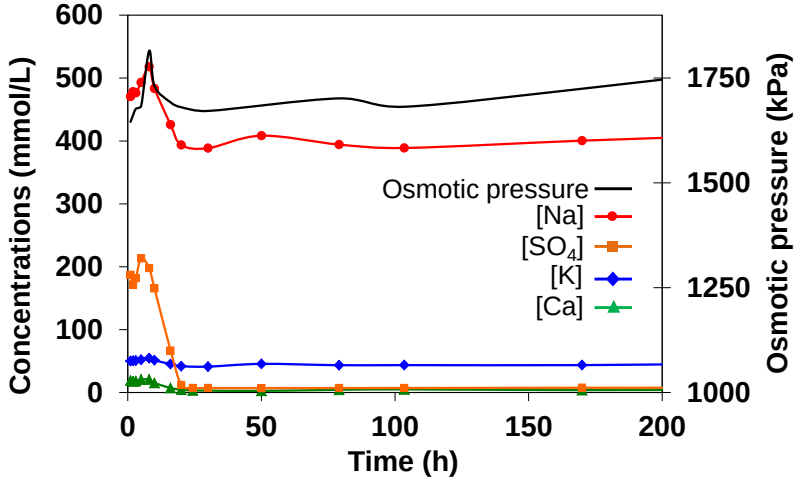

(a)

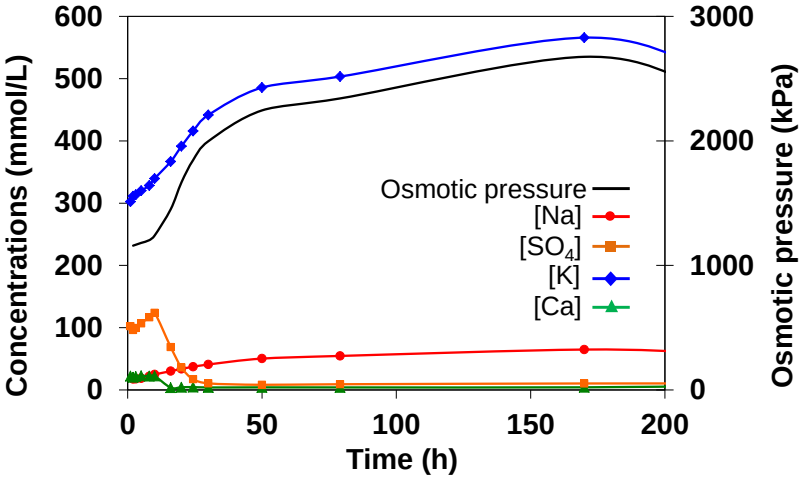

(b)

343 Figure 5: Evolution of the composition (Na^+, K^+, Ca^{2+}, SO_4^{2-}) and osmotic pressure of the interstitial

344 solution of CEM III/C cement pastes with (a) or without IERs (b).

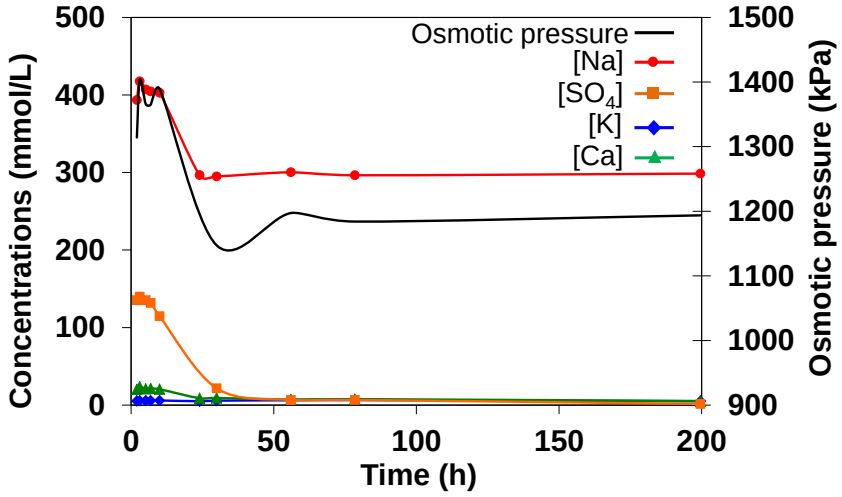

345

346 (a)

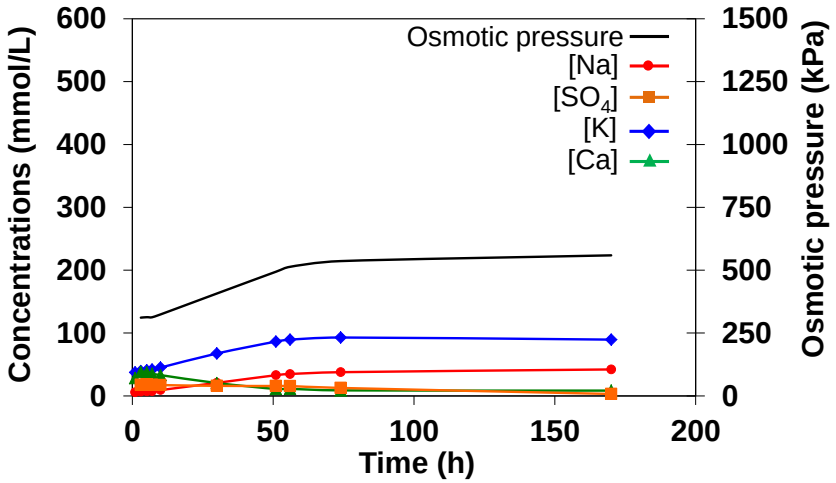

347

348 (b)

349

350

Figure 6: X-ray diffraction patterns of IERs-CEM I samples.

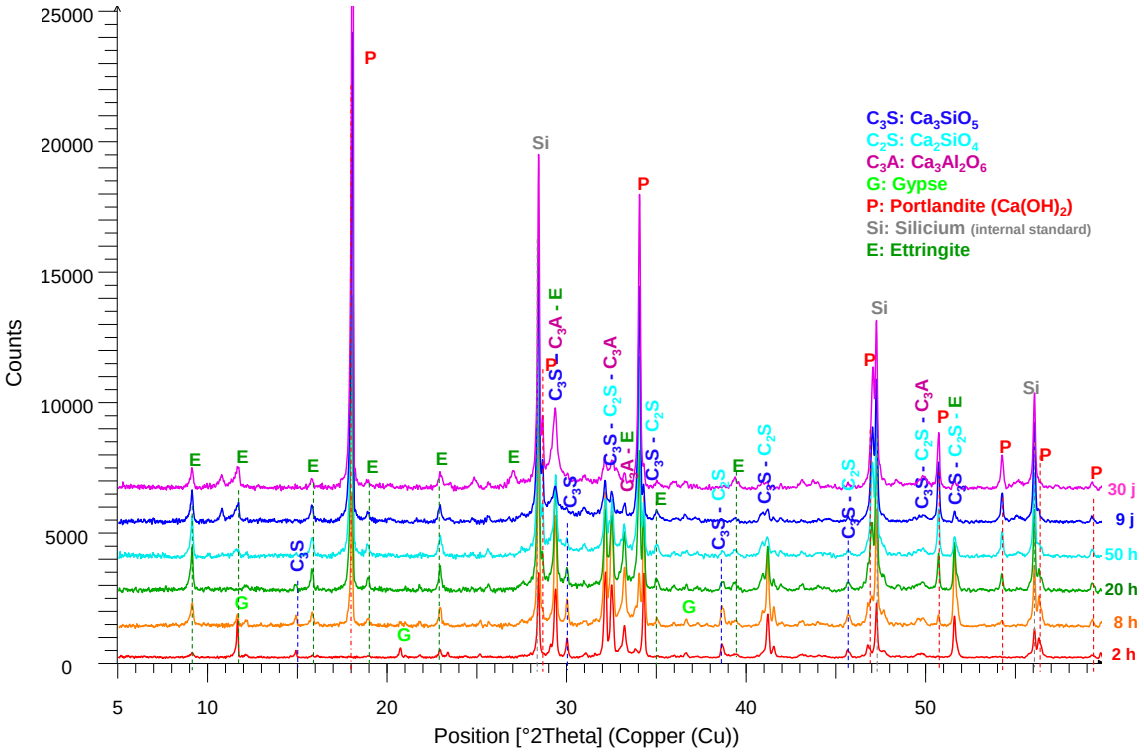

354 Figure 7: X-ray diffraction patterns of IERs-CEM III/C samples.

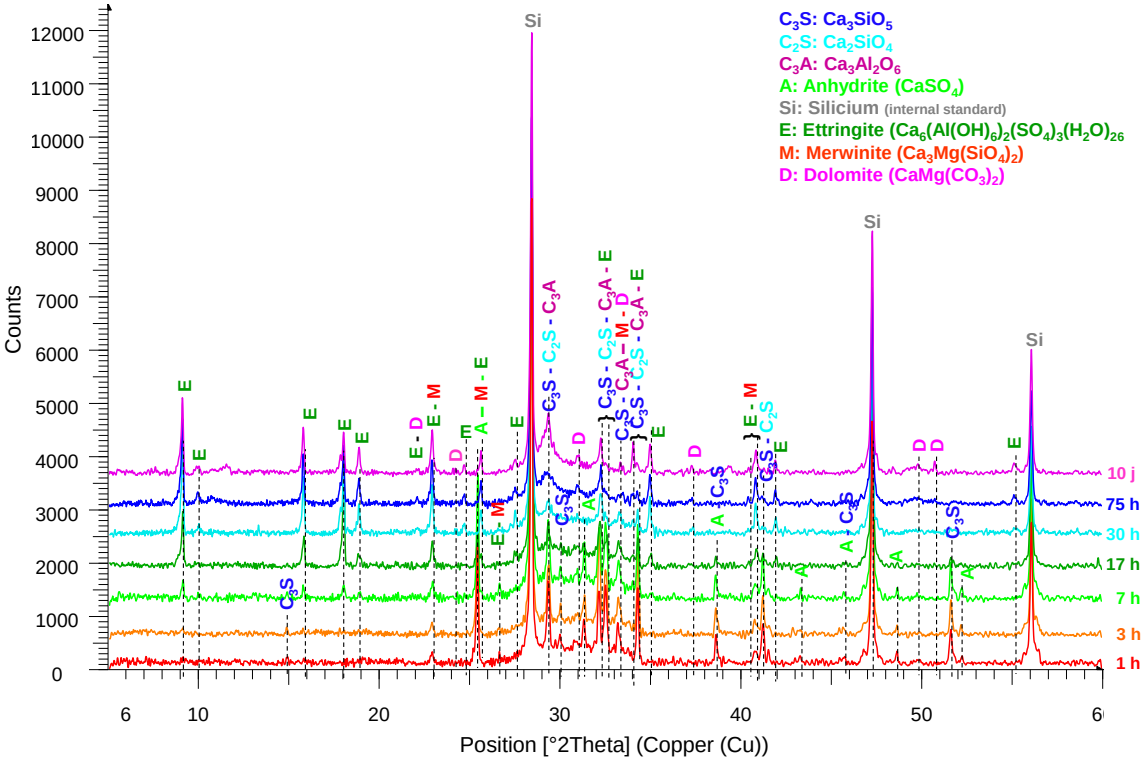

355

356

Figure 8: Influence of the resins on the phase content of CEM I (a) and CEM III/C (b) cement pastes during hydration.

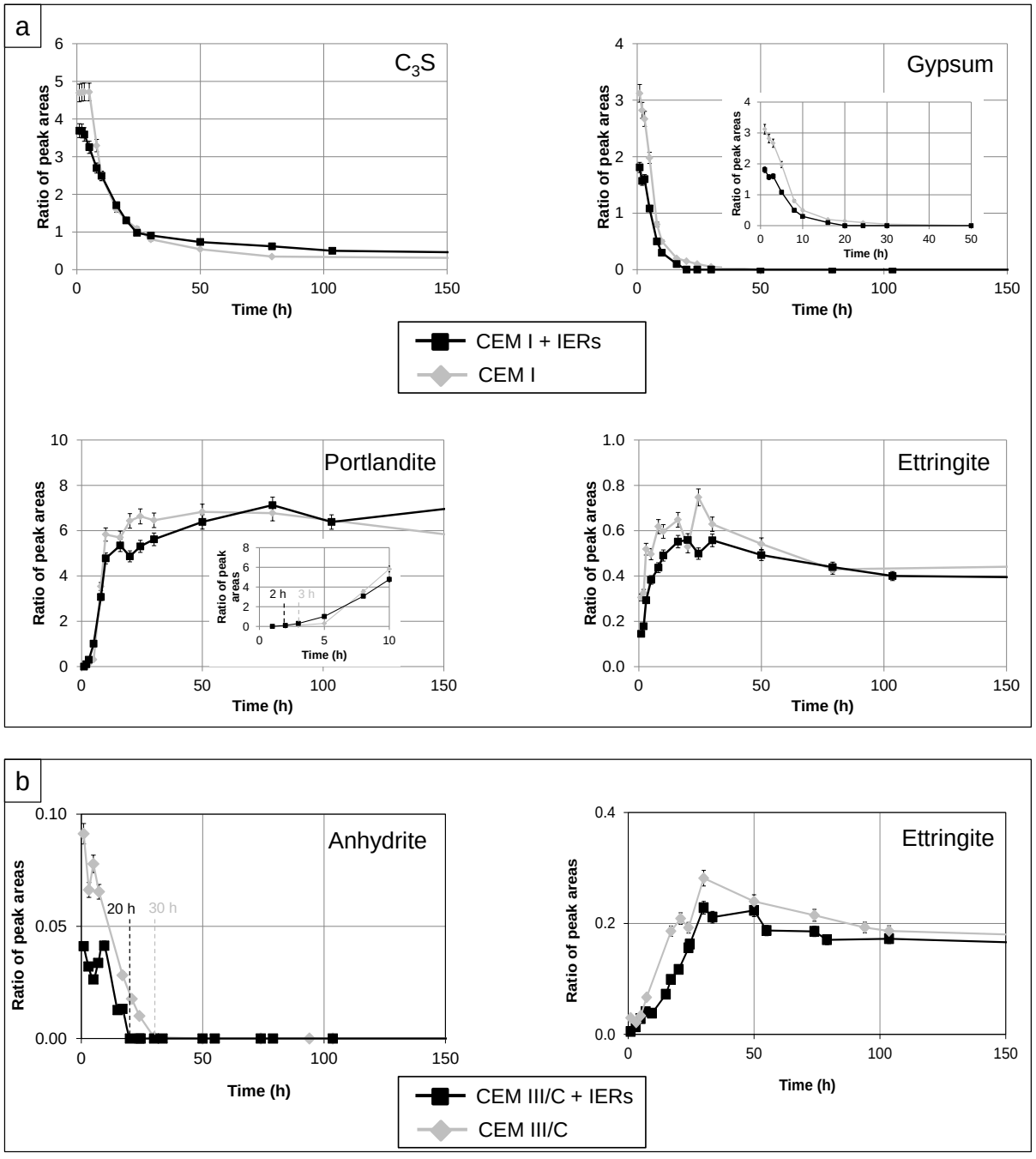

362 Figure 9: SEM observation of IERs-cement forms aged of 2 months: cavity previously occupied by a

363 resin bead. (a) CEM I sample; (b) CEM III/C sample.

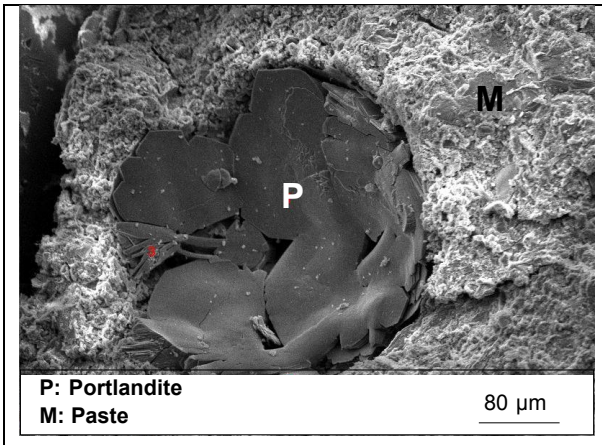

(a)

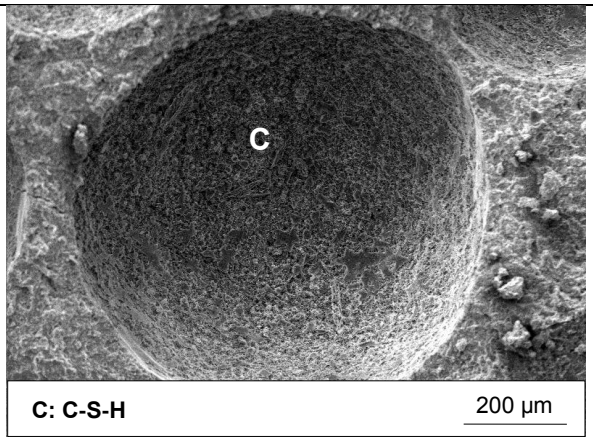

(b)

364

365

366 Figure 10: IERs-CEM I samples cured for 6 days at 25°C (left) or 5°C (right).

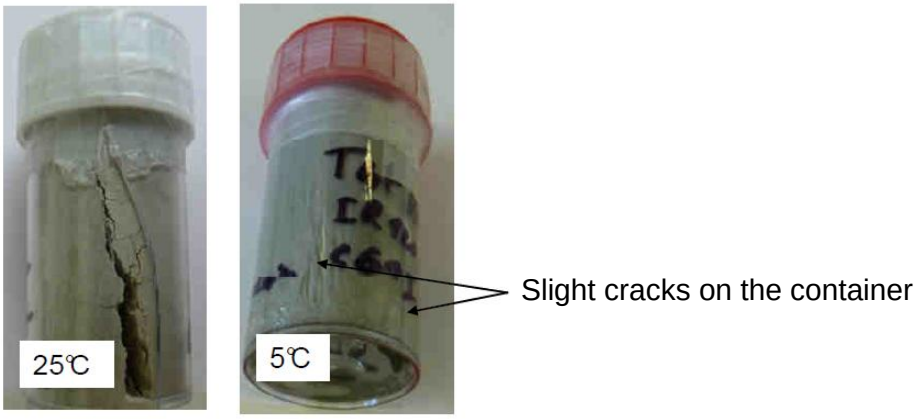

367

368

369

370 Figure 11 : Evolution of the interstitial solution composition (Na^+, K^+, Ca^{2+}, SO_4^{2-}) and Vicat needle

371 penetration versus time for IERs-CEM I samples cured at 5 and 20 °C..

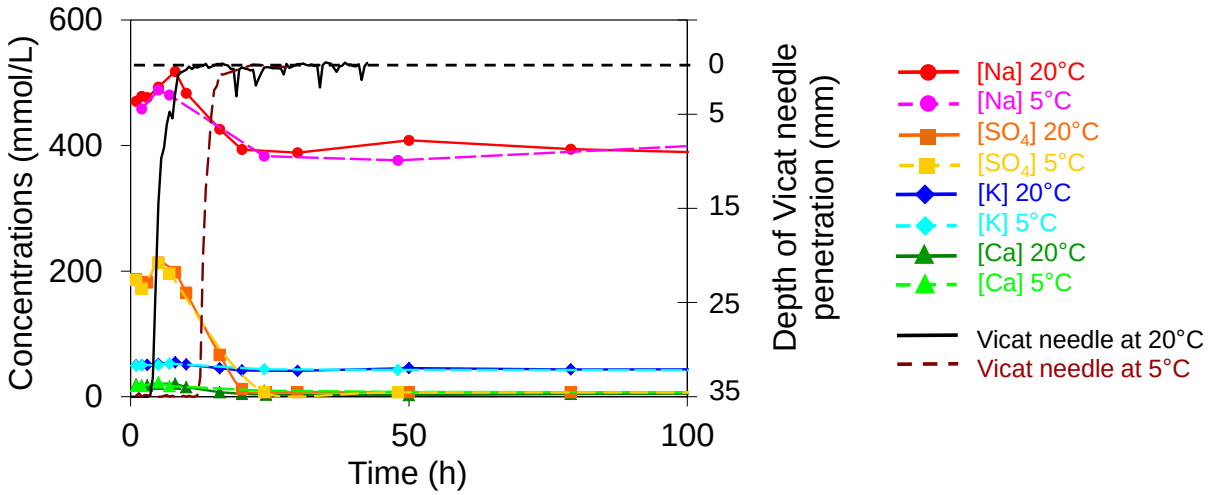

372